



Adjoint-based forecast sensitivity to quasi-geostrophic states during the rapid intensification of Typhoon Surigae (2021)

Nuo Chen¹, Michael Morgan¹

¹Department of Atmospheric and Oceanic Sciences, University of Wisconsin-Madison

Background and Motivation

The use of an adjoint model to calculate forecast sensitivities is more efficient than traditional sensitivity diagnosis involving “impact studies” (Errico 1995). While interpreting the sensitivity of a forecast response to individual state variables is trivial, such interpretations offer limited dynamical insight. Historically, the quasi-geostrophic potential vorticity (QGPV) “thinking” has been adopted to diagnose and interpret the mid-latitude synoptic weather system evolution. We have developed a method to calculate the sensitivity to quasi-geostrophic potential vorticity from the adjoint of the Weather Researching and Forecasting (WRF) model version 3.8. We reveal a relationship between the sensitivity to QGPV and the “balanced” sensitivity to winds and temperature under the QG constraint.

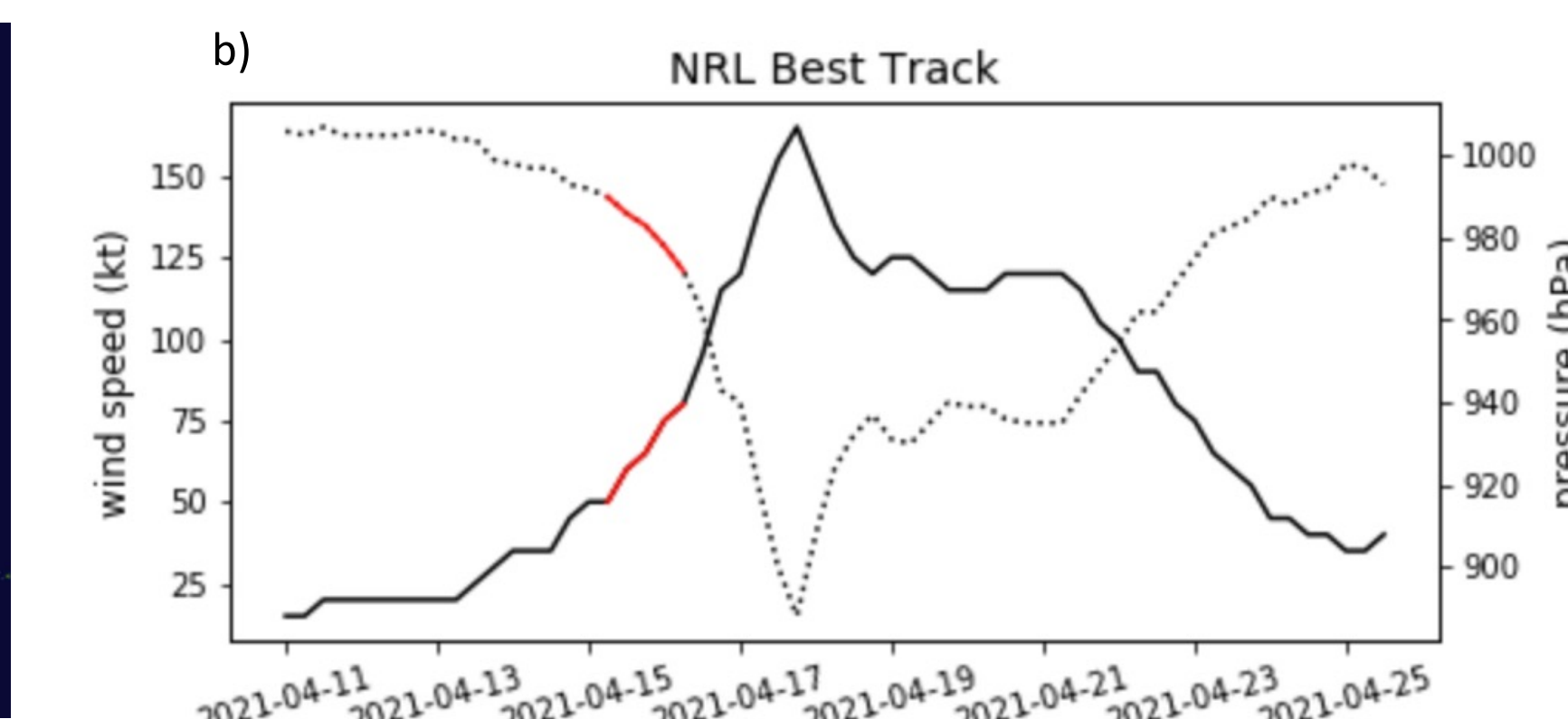
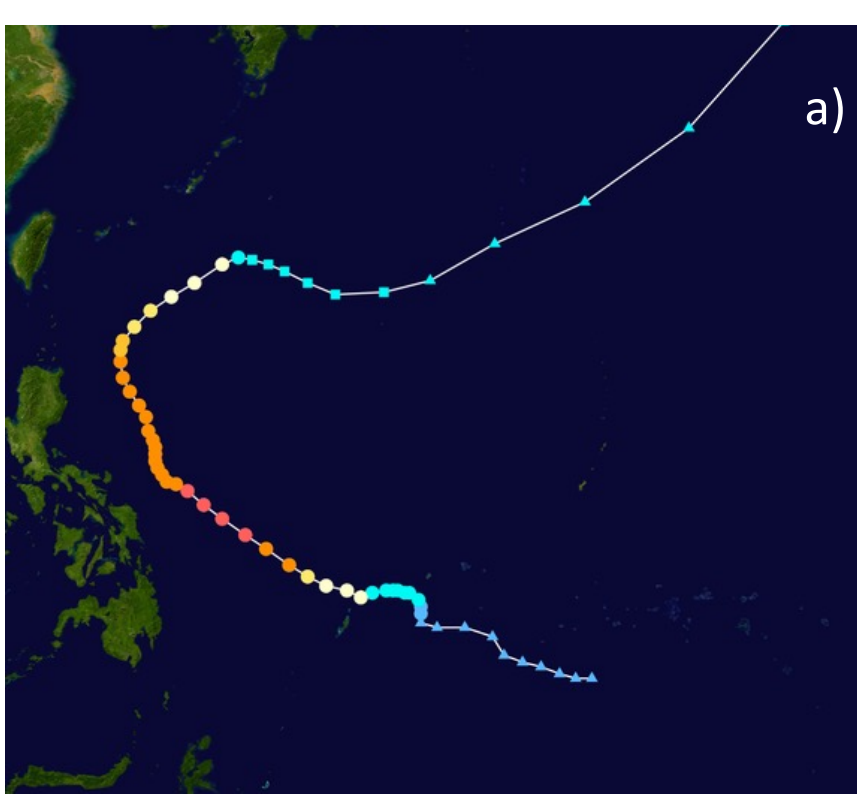
Using these sensitivities, optimal perturbations can be derived given the prescribed change in the final response function through minimizing the energy norm.

The goals of this presentation include:

1. Applying the sensitivity to QGPV in a tropical cyclone case and interpret the balanced sensitivity fields;
2. Comparing the unbalanced and balanced sensitivity outputs;
3. Prescribing the same amount of energy norm for optimal initial perturbations and comparing their difference in impacting the storm intensity.

Case Study: Super Typhoon Surigae (2021)

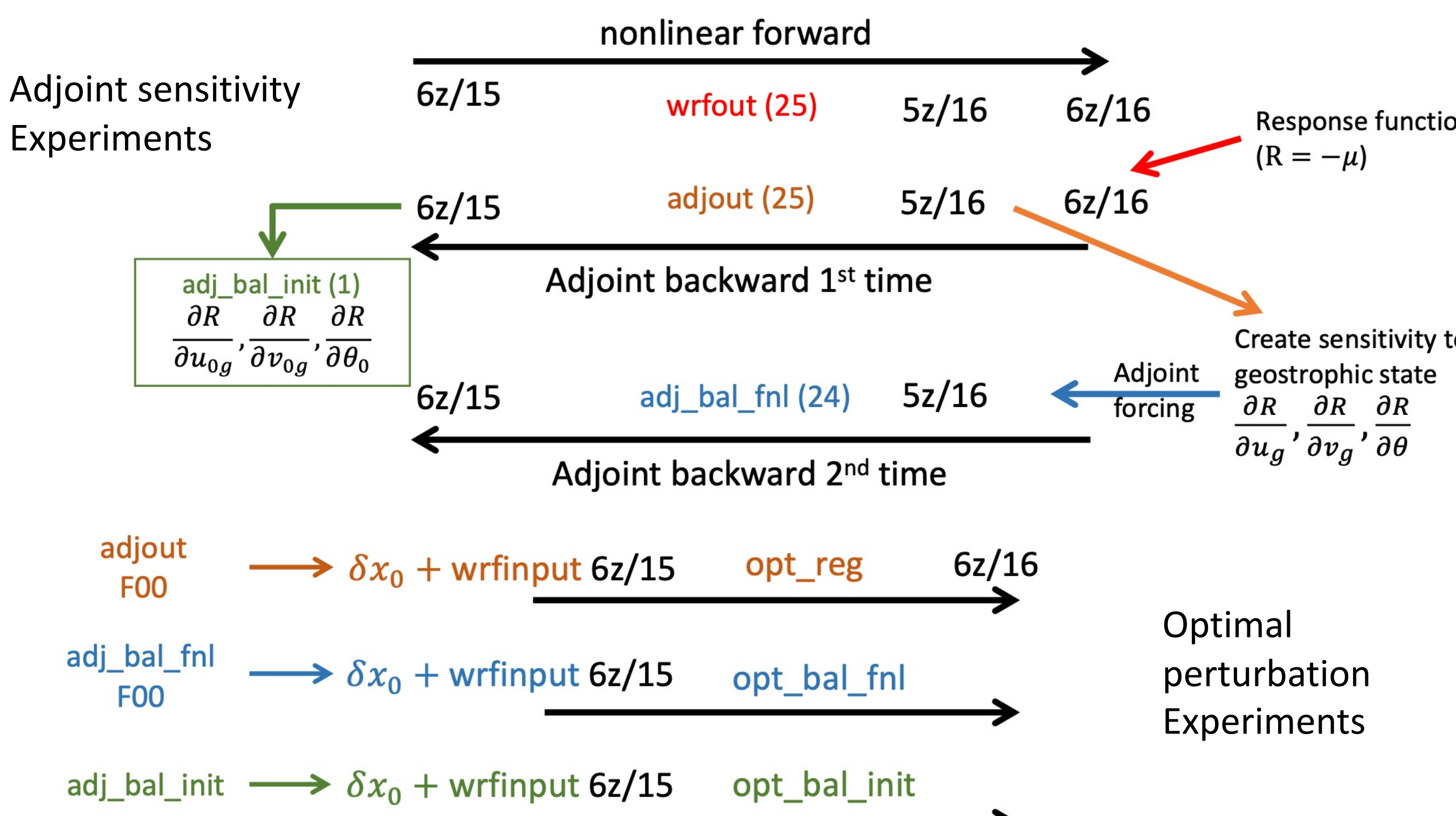
- Underwent RI (55 kt to 80 kt in 24 hours beginning 0600 UTC 15 April)
- Reached max wind at 1800 UTC 17 April with 120 kt max wind



Model Set Up

WRF-ARW V3.8.1 and its adjoint included in WRFPLUS V3.8.1

- Initialized with 0.25° GFS final analysis global data
- 24 km grid spacing and 41 vertical levels
- 24 hour forward non-linear and backward adjoint integration from 0600 UTC 15 April 2021 (F00; 6z/15) through 0600 UTC 16 April 2021 (F24; 6z/16)
- $R = -\bar{\mu}$ (column dry air mass) within the 995 hPa contour at 0600 UTC 16 April



Sensitivity to quasi-geostrophic potential vorticity (QGPV)

Start with formulating the optimal initial perturbation:

$$\Delta R = \left(\frac{dR}{dx}, dx \right) \text{ and } \delta x = (u', v', T')$$

Define an energy norm:

$$E = \frac{1}{2} \int_0^1 \iint_{\mathcal{R}} u'^2 + v'^2 + \frac{c_p}{T_{ref}} T'^2 d\mathcal{R} d\eta \\ = \frac{1}{2} \langle \delta x_0, W \delta x_0 \rangle \quad W = \begin{pmatrix} 1 & 0 & 0 \\ 0 & 1 & 0 \\ 0 & 0 & \frac{c_p}{T_{ref}} \end{pmatrix}$$

By forming and minimizing a Lagrangian L

$$\min_{\delta x_0, \lambda} \left(L = E + \lambda \left(\Delta R - \left(\frac{dR}{dx}, dx \right) \right) \right)$$

We can obtain the optimal initial perturbations and the Lagrange multiplier λ

$$\delta x_0 = \lambda W^{-1} \hat{x}_0^*, \quad \lambda = \frac{\Delta R}{\langle \hat{x}_0, W^{-1} \hat{x}_0 \rangle}$$

Similar to above, we can define a quasi-geostrophic pseudo-energy (E_{QGPV})

$$E_{QGPV} = \frac{1}{2} \int_{sfc}^{top} \iint_{\mathcal{R}} u'^2 + v'^2 + \frac{\gamma^2}{s} \theta'^2 d\mathcal{R} dp \\ = -\frac{1}{2f_0} \int_{sfc}^{top} \iint_{\mathcal{R}} q' \varphi' d\mathcal{R} dp \\ = -\frac{1}{2f_0} \langle q', \varphi' \rangle = \frac{1}{2} \langle q', W_q q' \rangle$$

Where the perturbation QGPV q' is defined as

$$q' = \varphi(\varphi') = \frac{\partial v_g}{\partial x} - \frac{\partial u_g}{\partial y} - \frac{\partial}{\partial p} \left(\frac{f_0}{s} \gamma \theta' \right)$$

$$E_{QGPV} = -\frac{1}{2} \left\langle q', \frac{\varphi^{-1}(q')}{f_0} \right\rangle = \frac{1}{2} \langle q', W_q q' \rangle$$

$$W_q = -\frac{1}{f_0} \varphi^{-1}$$

$$q' = \lambda W_q^{-1} \hat{q}$$

$$= \frac{\partial}{\partial x} (\lambda \hat{v}_g) - \frac{\partial}{\partial y} (\lambda \hat{u}_g) - \frac{\partial}{\partial p} \left(\frac{f_0 \gamma}{s} \lambda \hat{\theta} \right)$$

$$\hat{q} = -\frac{1}{f_0} \varphi^{-1} \left[\frac{\partial \hat{v}_g}{\partial x} - \frac{\partial \hat{u}_g}{\partial y} - \frac{\partial}{\partial p} \left(\frac{f_0 \hat{\theta}}{\gamma} \right) \right]$$

We define $\hat{u}_g, \hat{v}_g, \hat{\theta}$ as the QG balanced sensitivity field, and refer the original sensitivity outputs as unbalanced.

*For simplicity, denote $\partial R / \partial x$ as \hat{x}

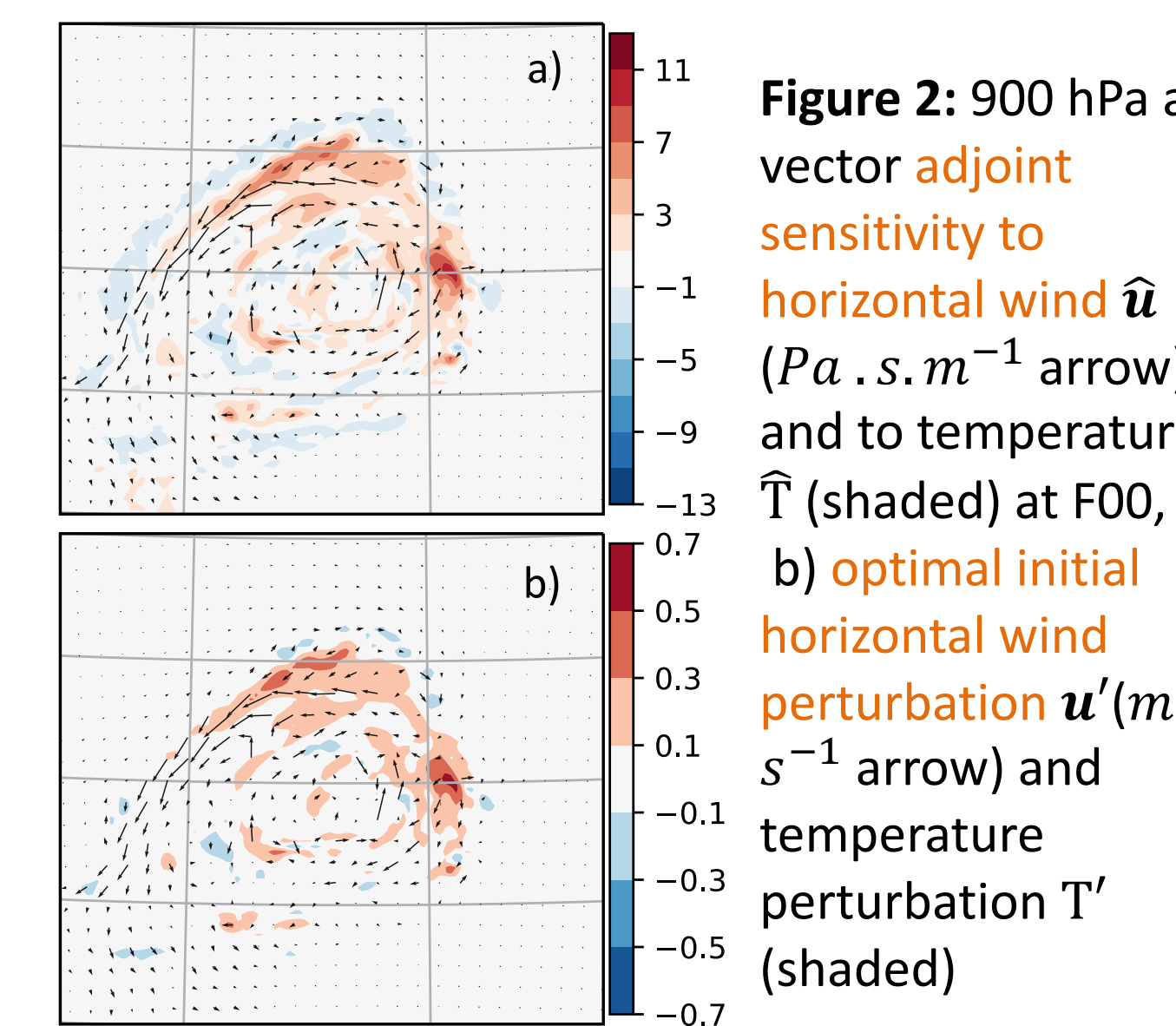


Figure 2: 900 hPa a) vector adjoint sensitivity to horizontal wind \hat{u} (Pa s m⁻¹ arrow) and to temperature \hat{T} (shaded) at F00, b) optimal initial horizontal wind perturbation u' (m s⁻¹ arrow) and temperature perturbation T' (shaded)

Optimal perturbation

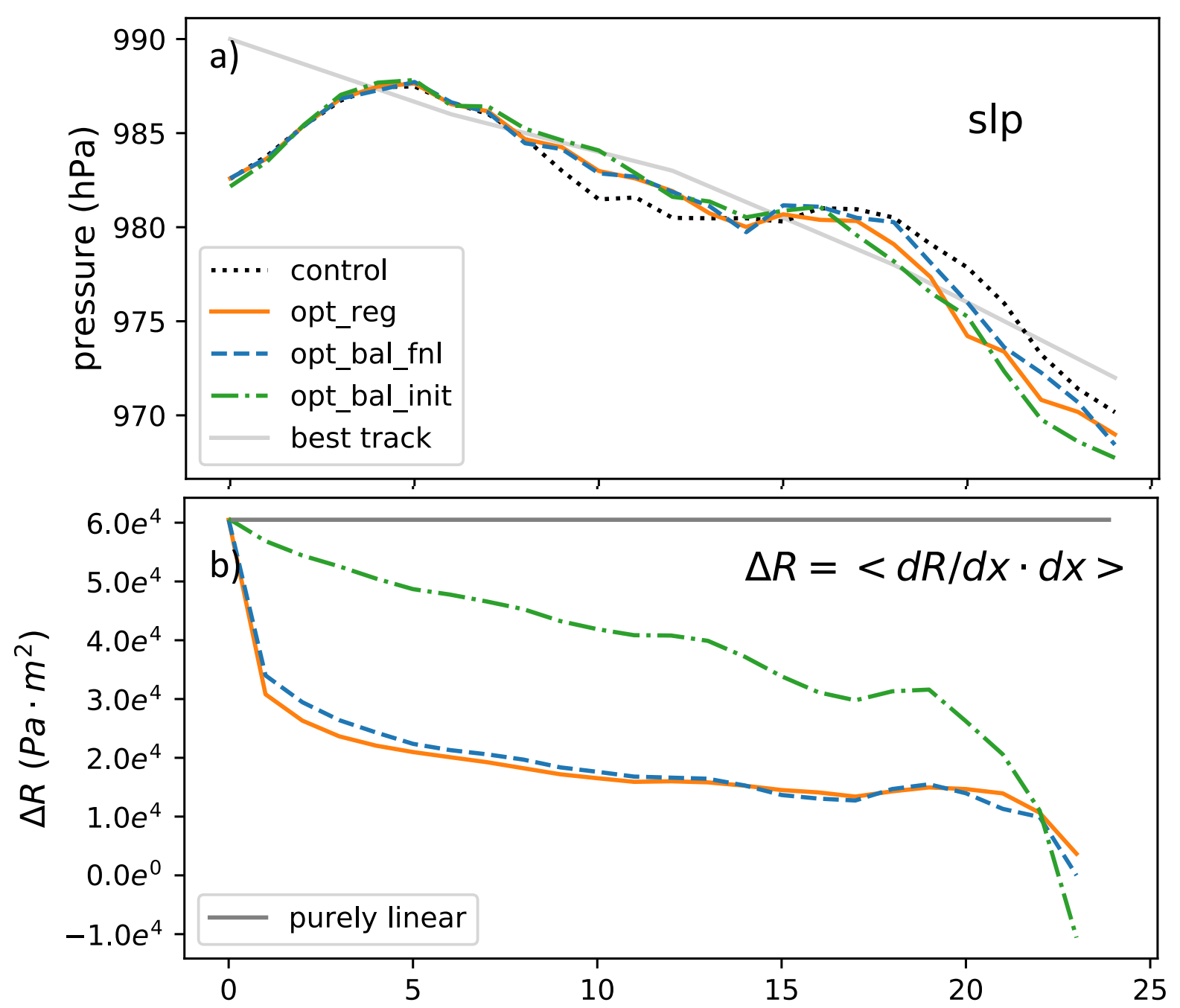
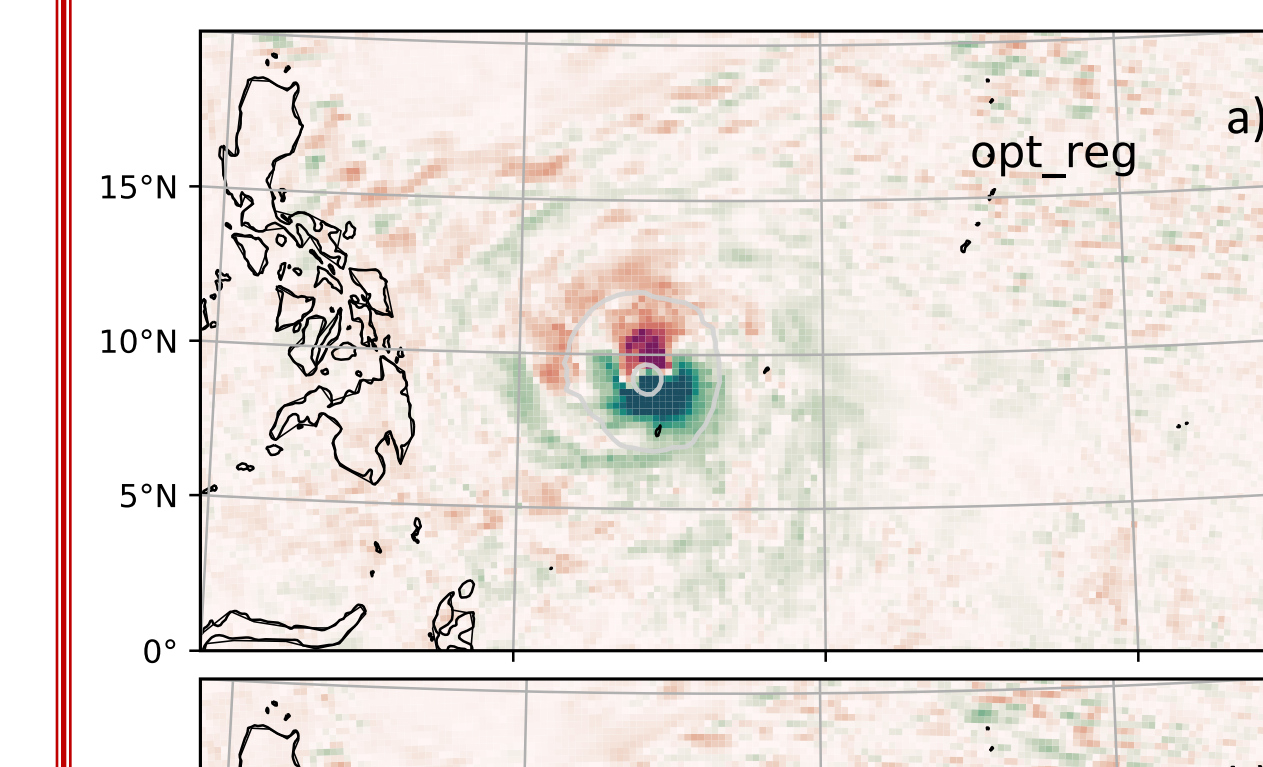


Figure 5: Optimal perturbation forward experiments initialized with optimal initial perturbations informed by adjoint (solid red), adj_bal_fnl (dashed blue), and adj_bal_init (dot-dashed green) and their differences in a) minimum sea level pressure of the storm, b) total change in response function $\Delta R = \langle dR/dx \cdot dx \rangle$

Optimal perturbation with no gravity wave feature at F00 is able to better intensify the storm in the response function area at F24;

If the experiment is absolute linear then ΔR should not change with time (gray line in Fig. 5b).

Optimal perturbations with gravity waves are speculated to be more nonlinear than balanced optimal perturbation.

The spatial distribution of changes μ in the domain at F24 is similar between the perturbation runs initialized with adjoint and adj_bal_fnl (Fig. 4a,b). The perturbation experiment initialized with balanced initial sensitivity field (Fig. 4c) produces a broader and more intense change in μ .

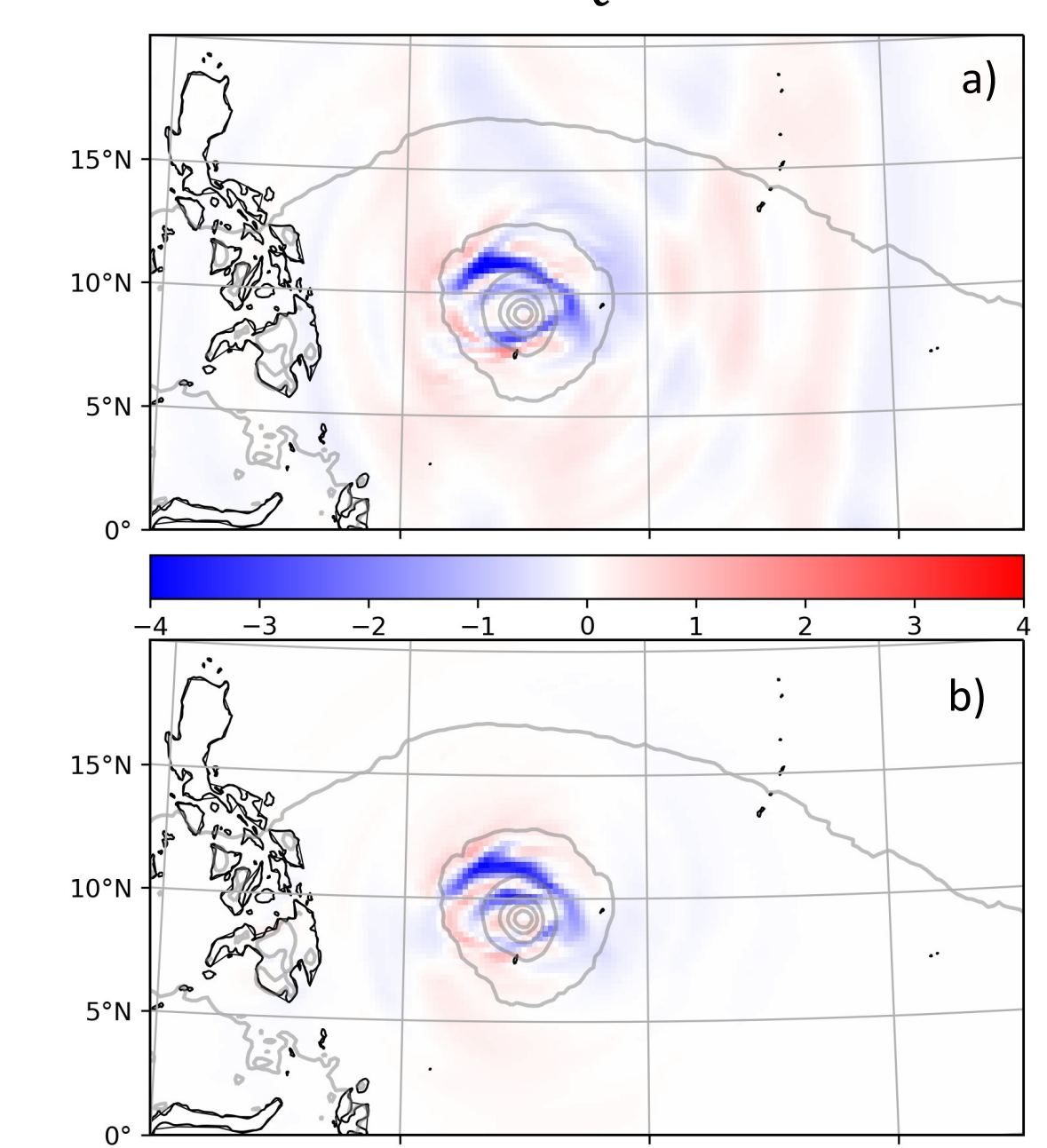


Figure 3: 900 hPa sensitivity to zonal wind (Pa s m⁻¹, shaded) and sea level pressure (contour) at F14 from experiments a) adjoint and b) adj_bal_fnl

The gravity wave pattern in a) which bounces back from the domain boundary in filtered out in (b), with the dominant feature mostly identical.

Sensitivity Analysis

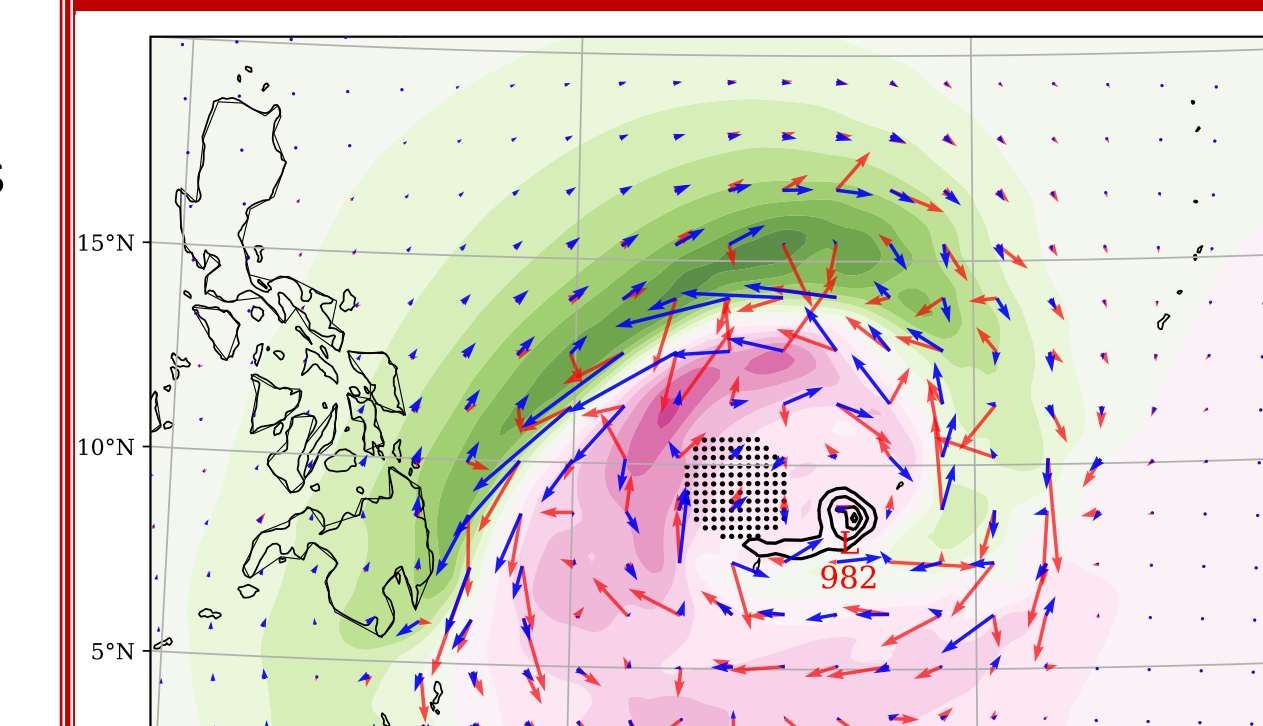
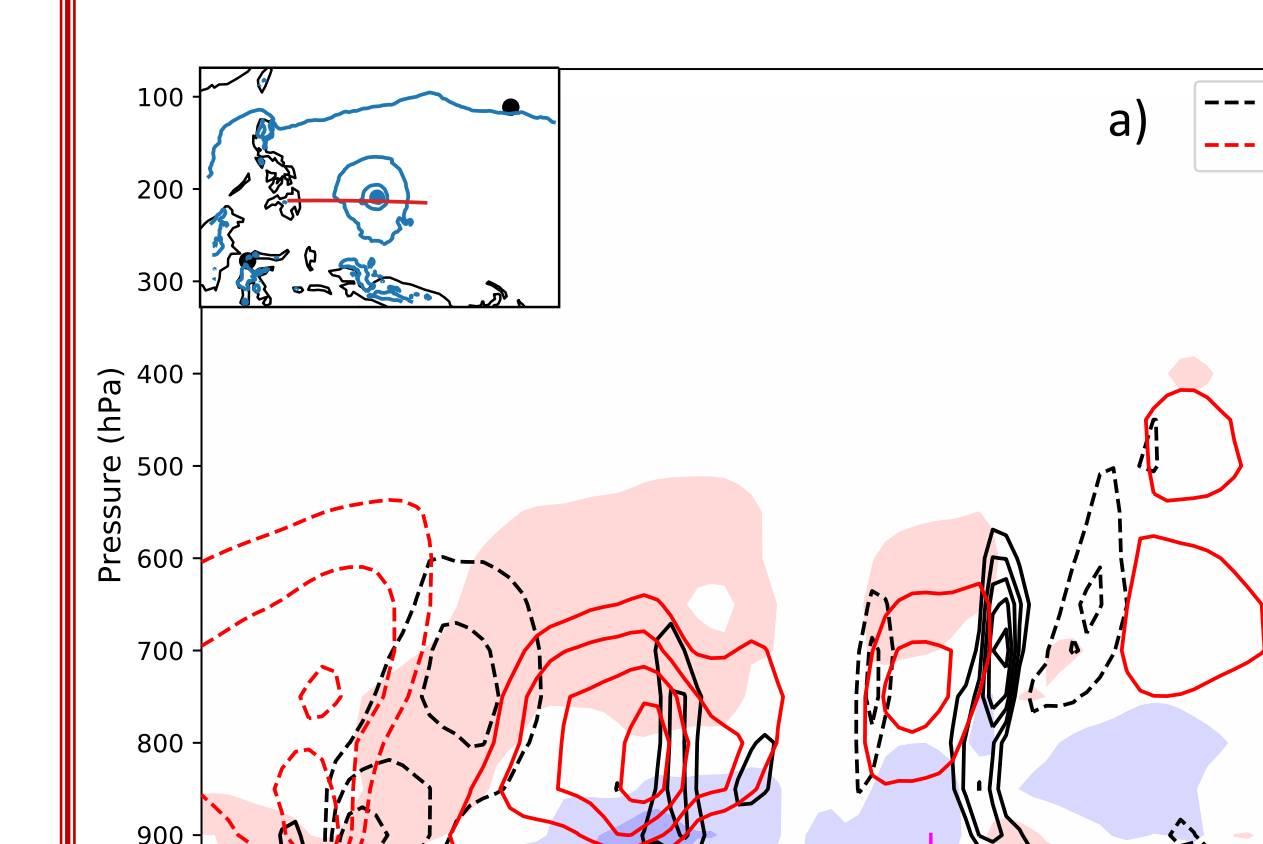


Figure 6: 900 hPa \hat{q} (Pa s; shaded), vector sensitivity to the geostrophically balanced horizontal winds \hat{u}_g (Pa s m⁻¹; blue arrows), to horizontal winds from adjoint \hat{u} (Pa s m⁻¹; red arrows) and background PV (contours; 10^{-5}s^{-1} interval) at 0600 UTC 15 April 2021 (F00). The response function used for this study is the column dry air mass ($-\mu$) in the meshed area (slp < 995 hPa at F24).



More QGPV (pink) further northwest to the response function area is favored to deepen the storm 24 hours later in mesh area

Fig. 6 shows that there is huge difference between the balanced and unbalanced sensitivity field near the storm center, the unbalanced sensitivity has more divergent feature.

Figure 7: QG balanced sensitivity cross sections from adj_bal_init at 0600 UTC 15 April 2021 (F00) a) sensitivities to geostrophic meridional winds \hat{v}_g (black contours; 0.4 Pa s.m^{-1} interval), to balanced potential temperature $\hat{\theta}$ (Pa K⁻¹, shaded) and to QGPV \hat{q} (Pa s; red contour) b) balanced \hat{v}_g (black contours); unbalanced \hat{v} (yellow contour), and meridional wind speed v from wrfout (m s⁻¹; shaded)

A positive sensitivity to QGPV \hat{q} is surrounded by cyclonic vector sensitivity to winds \hat{u} , with a positive sensitivity to potential temperature $\hat{\theta}$ above and a negative $\hat{\theta}$ below (Fig. 7a);

Fig. 7b shows the \hat{v}_g can catch most of \hat{v} 's characteristics, but missing a few boundary layer and inner core features

Future Work

- Develop the sensitivity to Ertel PV which is more general and applicable in the tropics and interpreting the tropic cyclone dynamics;
- Investigate the gravity wave's general impact on the change in response function in optimal perturbation experiments;
- Explore the role of imbalance in tropical cyclone development

Acknowledgements

This study was supported by the Space Science Engineering Center/Cooperative Institute for Meteorological Satellite Studies.